# Autonomous Mobile Robot for Outdoor Slope Using 2D LiDAR with Uniaxial Gimbal Mechanism

**Shunya Hara[*1], Toshihiko Shimizu[*1], Masanori Konishi[*1], Ryotaro Yamamura[*1], Shuhei Ikemoto[*2]**

[*1]Kobe City College of Technology, 8-3, Gakuen-Higashimachi, Nishi-ku, Kobe, 651-2194, Japan
Email: r115159@g.kobe-kosen.ac.jp

[*2] Graduate School of Life Science and Systems Engineering, KyusyuInstitute of Technology, 2-4 Hibikino, Wakamatsu, Kitakyushu, Fukuoka, 808-0196, JAPAN

**The Nakanoshima Challenge is a contest for developing sophisticated navigation systems of robots for collecting garbage in outdoor public spaces. In this study, a robot named Navit(oo)n is designed, and its performance in public spaces such as city parks is evaluated. Navit(oo)n contains two 2D LiDAR scanners with uniaxial gimbal mechanism, improving self-localization robustness on a slope. The gimbal mechanism adjusts the angle of the LiDAR scanner, preventing erroneous ground detection. We evaluate the navigation performance of Navit(oo)n in the Nakanoshima and its Extra Challenges.**

**Keywords:** mobile robot, ROS, LiDAR, SLAM, uniaxial gimbal mechanism, slope

## 1. Introduction

Public events such as the Tsukuba Challenge (see supporting material A) and the Nakanoshima Challenges (supporting material B and C) are organized for demonstrating the outdoor public space navigation potential of robots. In addition to the driving of the Tsukuba Challenge, those of Nakanoshima involved collecting garbage. The garbage collection task includes object recognition, pickup, transportation, and driving in a natural terrain. For utility, the garbage pickup robot must patrol the cleaning area without colliding with pedestrians and other obstacles.

A robot moving in coexistence with humans in an environment requires an appropriate size and weight and a speed comparable to walking, among others. Compared to an automotive car (see supporting material D), the small robot size is a resource constraint; the robot cannot contain many sensors or a large computer. Therefore, a simple, compact, lightweight, and robust system is desirable. In this study, we introduce a garbage pickup robot integrating a pickup and transport system with driving. We then explain the design and development of the Navit(oo)n, which handles the autonomous mobility slope problem as illustrated in **Fig. 1**, with the manufactured robot shown in **Fig. 2**.

At the 2018 World Robot Summit (henceforth WRS), the pickup and transport strategy were highlighted to simplify pickup planning by end effectors and reduce system development loads by utilizing open-source

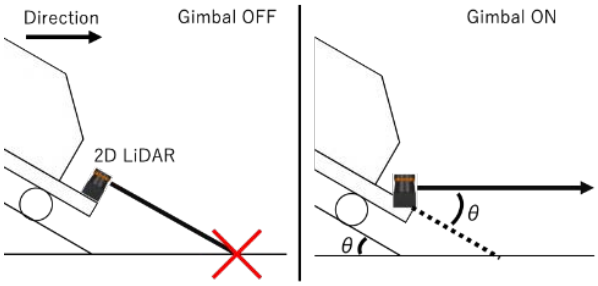


**Fig. 1. Uniaxial gimbal mechanism for slope.**


**Fig. 2. Navit(oo)n overview.**

software [1, 2]. Especially, soft robot grippers [3, 4] such as granular material-based jamming grippers attracted attention as simple end effectors for multiproducts collection [5–8]. Regardless of an object's posture, the robot grasps the object by a negative pressure switch, making it suitable for garbage pickup involving limited resources. Moreover, a jamming gripper strengthening the negative pressure adhesion was developed, and multiple grasps now exist [9, 10]. Therefore, we produce a system with a jamming gripper involving multiproducts collection system [1, 2] with considering simplification efforts. Here, to produce an outdoor garbage pickup robot, the selection and concentration on the development load are most important.

Thus, considering the Tsukuba Challenge development policy [11], our outdoor autonomous mobile system involves the following features: (1) 2D LiDAR with the uniaxial gimbal for a wide field of view and robust slope sensing, (2) high-precision odometry with gyro sensing, (3) appropriate wheels for ascending in the outdoor environment, (4) self-localization by map matching and particle filtering, and (5) image feature and

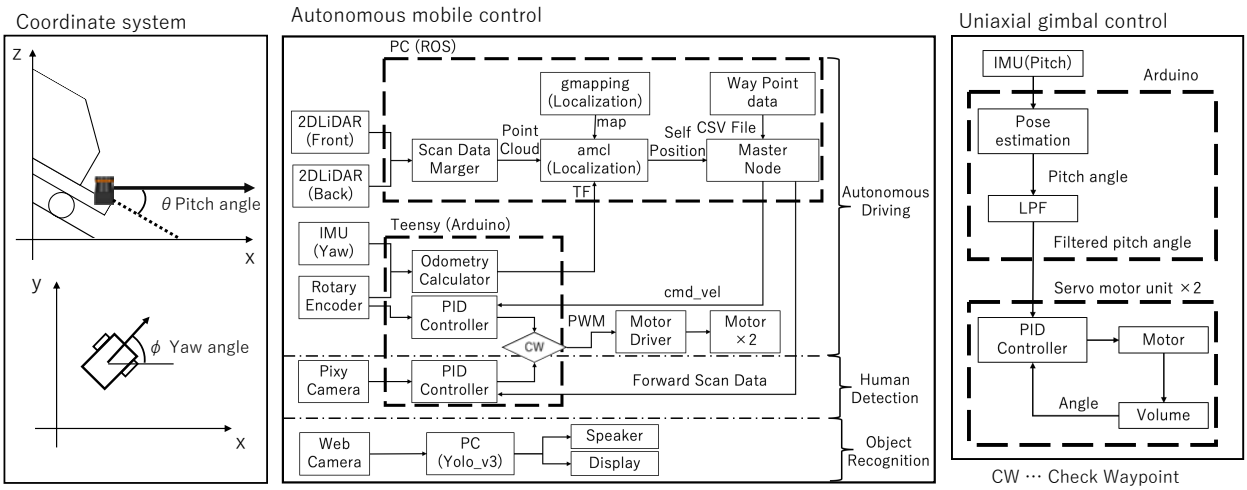


**Fig. 3. System diagram of Navit(oo)n. The coordinate system is shown in the left figure. The upper figure shows a robot on the slope with the travel and vertical direction on the x and z-axis, respectively. $\theta$ denote the pitch correction angle by the gimbal. The lower left figure shows a two-dimensional plane viewed from the top, and yaw angles are expressed in $\phi$. The system diagrams of autonomous mobile and uniaxial gimbal control are shown in the center and right figures, respectively. Note that the IMU for gimbal corrects only the pitch angle, while the IMU for autonomous mobile deals only with the yaw angle.**

object recognition under outdoor illumination. The proposed system contains tiny, inexpensive, and pervasive sensors that can be mounted easily in other mobile robots.

The 2D LiDAR detects the ground on the slope, as illustrated in **Fig. 1**, which degrades the robot's self-localization. In previous studies, a 2D LiDAR method employed as 3D by oscillation with a motor was proposed [12]. Although this system is proven as stable in outdoor operation, its annual developmental load remains a limitation. Besides, a method for 2D map creation with height information beforehand using 2D LiDAR, accompanied by height-based autonomous mobile, was also advanced [13]. However, this method requires additional sensors, with its computational cost expected to increase during driving on flat areas. Although some SLAM packages provided by ROS removes false detection components (such as the ground) from the LiDAR's measurement data, these software approaches may fail to estimate self-location by over-removing features, such as a pole and fence. Therefore, in this paper, we consider a hardware approach avoiding the ground detection by increasing the quality of the measurement itself. Thus, we simplify the slope problem during the robot's straight track movement, with inclination avoided by adjusting the scanning plane of the 2D LiDAR to the horizontal plane. The driving performance of Navit(oo)n (**Fig. 2**), which involves the uniaxial gimbal mechanism, is verified through participation in the Nakanoshima 2019 and the Nakanoshima 2019 Extra Challenges.

## 2. NAVIT(OO)N: A ROBOT ADAPTED TO THE NATURAL TERRAIN

The Nakanoshima Challenge is an open event for testing the performance of robots in a public environment in coexistence with people. The three tasks for the robots involved are as follows:

1. The robot travels 475 m around a defined course.
2. The robot detects persons standing in two areas to collect the garbage.
3. The robot distinguishes between PET bottles, cans, and lunch boxes, with the three objects individually provided by a person.

**Table. 1 Machine specifications.**

| | | |
|---|---|---|
| Weight | 43 kg | |
| Size | 1000 mm×750 mm×800 mm | |
| OS | Main PC: Ubuntu 16.04 for ROS<br>2nd PC: Ubuntu 16.04 for Yolo_v3 | |
| Software | ROS, Arduino IDE | |
| Sensor | 2D LiDAR×2<br>3D LiDAR<br>IMU<br>Camera<br>Rotary encoder | UTM-30LX<br>YVT-35LX<br>MPU6050<br>Pixy Cam<br>AMT102-V |
| Tires | 6-inch tires | Honda Monkey |
| Input | PS3 controller, mouse, keyboard | |
| Output | Motor (RS-775), display, speaker | |
| Power | Li-ion battery (DC24V 5.2Ah) ×2 (62KSP545483-2). One for motor, and the other for sensors.<br>Mobile Battery (AC110V 434Wh) (Anker PowerHouse) for PCs. | |

**Table 1** presents the specifications for Navit(oo)n, which include 6-inch tires like those for motorcycles, enabling the robot to overcome various steps. The robot also contains a rotary encoder on each tire for recording the travel distance. Besides, the system is equipped with 2D LiDARs at the front and rear for measuring all around the robot.

**Fig. 3** illustrates the connection between the hardware and software of Navit(oo)n. In this figure, CW stands for Check Waypoint and switches the behavior according to the type of waypoint in autonomous mobile. The details are described in chapter 4. We had the 3D LiDAR on

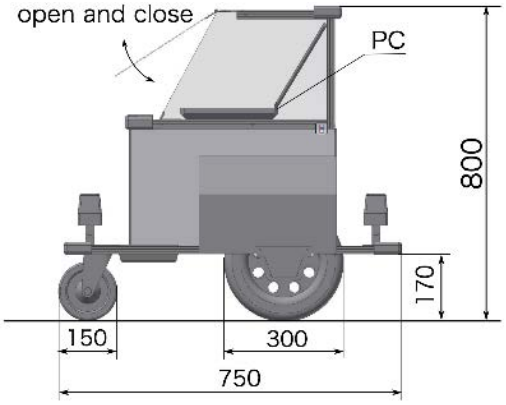


Fig. 4. Side view of Navit(oo)n.

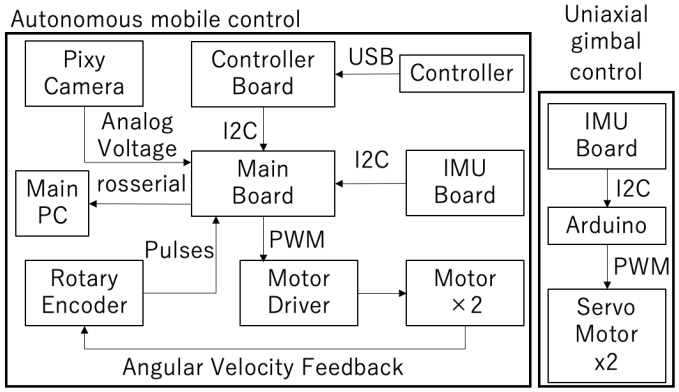


Fig. 5. Electrical relationship.

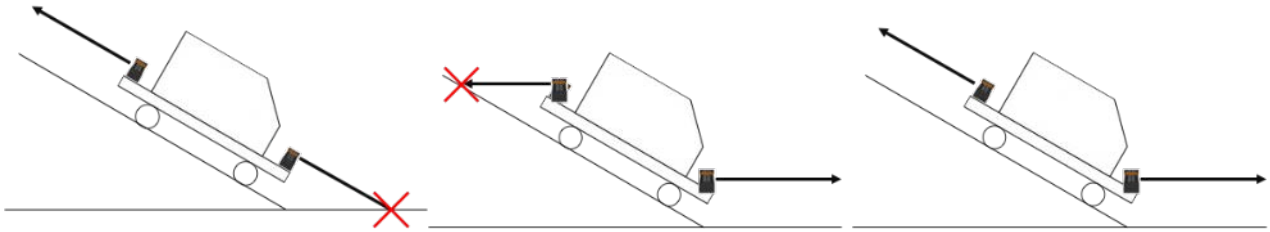

(a) Frontal failure. (b) Rear-side failure. (c) Proposed approach.

**Fig. 6. Demonstration of the LiDAR sensing on a slope during downhill movement involving the uniaxial gimbal.**

Navit(oo)n, but the scanning length of the 3D is limited, and the slope problems with 2D LiDAR is our main concern, therefore we mainly consist our system by 2D as the following paragraph.

### 2.1. Mechanical characteristics of Navit(oo)n

The rotary encoders in the tires provide feedback on the distance travelled by the robot. The error associated with turning diminishes with decreasing tire diameter; if the tire's diameter is too small, the robot may be unable to run oversteps. We discussed this trade-off with teams that participated at the Nakanoshima Challenge. These teams recommended 300-mm-diameter motorcycle tires as driving wheels and 150-mm-diameter tire casters as auxiliary wheels. **Fig. 4** displays the dimensions of various parts of the robot.

To quickly adjust and check the system during the experiment, the main control PC for the ROS is placed in the robot's upper area. Moreover, to enhance the visibility of the control PC, we utilized a transparent acrylic plate a s the cover. Moreover, the robot is waterproof, with plastic cardboard, involving sealing tape, covering the lower part. The waterproof cover can be quickly opened and closed; the battery and the control circuit in the lower part are also accessible.

An OpenManipulator-X, with a short reach of 380 mm, is at the robot's bottom for collecting garbage from the ground. As the end effector, we utilized the universal vacuum gripper (UVG) [9], which is a vacuum suction cup with a deformable lip and comprising a jamming gripper that captures uneven shapes. Therefore, the UVG handles various uneven objects with its simple structure through suction. However, Navit(oo)n presently lacks the robot arm and UVG due to developmental schedule limitations.

### 2.2. The electrical circuit of Navit(oo)n

The expected functions of Navit(oo)n's electronic circuitry depicted in **Fig. 5** are as follows:

1) Controlling two motors for autonomous mobile
2) Retrieving the rotary encoders and IMU data
3) Ensuring reliable odometry
4) Providing a wired or wireless connection to a human-operated controller

We designed the circuit to perform these functions through Eagle CAD and fabricated it using a board processing machine. An I2C connects the main, controller, and IMU boards, with the main board working as the master, while the others are slaves.

Pulse-width modulation (PWM) from the main board controls the motor driver (Cytron MD30C). A DC–DC converter (MPM80) steps down from 24V to 12V for the main board, while others reduce the voltage to 5V for the other boards. We used an Arduino-compatible Teensy 3.5 microcontroller for the main board and rotary encoders, requiring high processing power.

## 3. Uniaxial Gimbal Mechanism for Outdoor Slope

False ground detection by the 2D LiDAR, as shown in **Fig. 1**, adversely affects self-localization. Therefore, Navit(oo)n contains 2D LiDARs with the uniaxial gimbal mechanism.

### 3.1. Uniaxial gimbal control

The uniaxial gimbal mechanism maintains the 2D LiDAR parallel to the horizontal plane. The system configuration of the uniaxial gimbal mechanism is described. It was designed to be completely independent of other autonomous movement systems and to function as a piece of hardware. This system consists of a servo motor unit, an Arduino control unit, and an IMU, as shown in **Fig. 3**. The electrical relation of the gimbal control is shown in **Fig. 5**. First of all, the robot's posture is obtained by integrating the 3-axis angular velocity obtained from IMU with Arduino. Then, the time sequence of the angular velocity is calculated by the moving average method to posture angles. Since the uniaxial gimbal mechanism operates only at the pitch angle, only that angle is taken from the calculated posture and passed through a low-pass filter. The filter reduces the response of the gimbal mechanism to the intention in order to reduce the noise caused by vibration during the run. The filtered pitch angle is sent to the servo motor unit as a reference value. The servo motor unit uses an inexpensive hobby servo and has a built-in variable resistance motor angle reading and feedback system. The gimbal mechanism involves a set motion range, preventing nonparallel inclination to the body. This range limitation prevents the LiDAR from touching the ground, as shown in **Fig. 6(a)**.


**Fig. 7. Overview of uniaxial gimbal.**


**Fig. 8. Uniaxial gimbal test.**

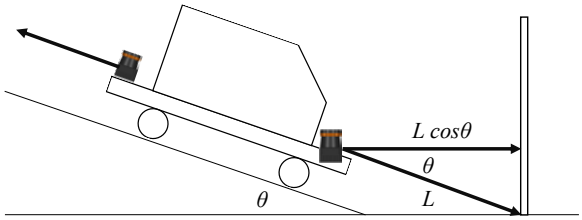


**Fig. 9. Uniaxial gimbal test.**

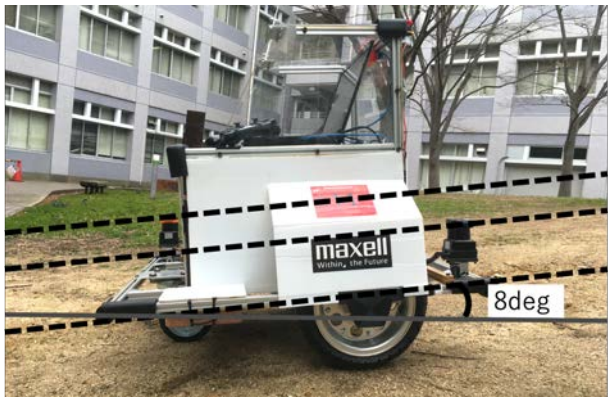


(a) Without gimbal control.


(b) With gimbal control.

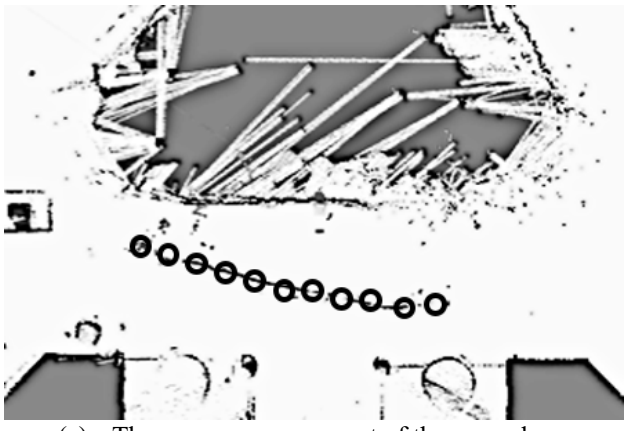

(c) The wrong measurement of the ground.

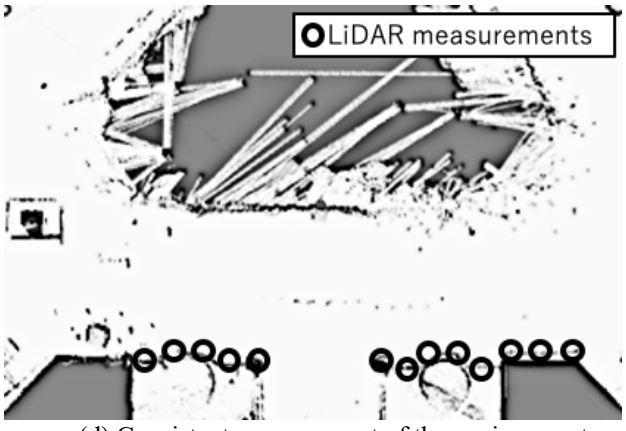


(d) Consistent measurement of the environment.

**Fig. 10. LiDAR sensing on an slope with and without the uniaxial gimbal control.**

Next, we explain the slope strategy of the gimbal mechanism. The 2D LiDARs of Navit(oo)n with the proposed gimbal mechanism enable 360-degree view of the robot. In the absence of the gimbal mechanism, the LiDAR on the lower slope side touches the ground, as shown in **Fig. 6(a)**. If the mechanism simply maintains the LiDAR horizontal, that on the high side hits the rear ground, as depicted in **Fig. 6(b)**. Therefore, the lower slope side's gimbal retains the LiDAR parallel to the horizontal plane, while the upper side's LiDAR is parallel to the slope (**Fig. 6(c)**). As such, the front and rear LiDARs operate synergistically on the slope to prevent a localization error. As displayed in **Fig. 7**, the gimbal involving a servomotor is a simple structure, with testing on the real robot exhibited in **Fig. 8**.

Note that the autonomous mobile system only manages its yaw angle as shown in **Fig. 3**, and it measures the horizontal distance by the uniaxial gimbal mechanism during running on the slope. Therefore, the environment map generated by the system is the deformed map shortened the measurement distance between the robot on the slope to obstacles. Figure 9 shows the measurement of the robot on the slope detecting an obstacle. Let $L$ be the measurement distance to the obstacle by LiDAR without the gimbal, then with the gimbals, the distance is $Lcos\theta$, which is shorter than $L$, because the gimbal always face to the obstacles perpendicularly.

The problem of this shortening measurement is considered to be relatively small compared with the localization error by the false detection of the ground, because the robot perceives the world in the deformed coordinate system both at the stage of generating the map and autonomous movement. However, there is a possibility that correction of the map distortions may be required when using the GPS and loop closing process of the environmental map, and this problem is considered as the future work.

Additionally, the gimbal pitch rotation physically changes the position and orientation of the 2D LiDAR, and the change is not managed by the ROS TF, but the recognition was not affected by this rotation as shown in later section.

### 3.2. Experiments with the uniaxial gimbal

We tested the operation of the uniaxial gimbal mechanism in the courtyard of the mechanics department building in Kobe City College of Technology. The robot runs with the uniaxial gimbal activated produce an environmental map from the ROS system, as shown in **Fig. 11**. The courtyard involves a hill at its center, and the robot was tested on the slope.

We compared data measured by the 2D LiDARs on the slope with and without the uniaxial gimbal control. When the gimbal control is deactivated (**Fig. 10(a)**), both LiDARs are parallel to the slope, whereas when activated (**Fig. 10(b)**), the front side's LiDAR is parallel to the slope, while that at the rear is oriented identical to the horizontal plane. The black and dot lines depict the horizontal and slope line, respectively. Measurements involving the gimbal control activation and deactivation using Rviz are illustrated in **Fig. 10(c)** and **(d)**, with dots highlighting measured data. Without the control, the dots are scattered around the ground, while with the control, the measured data are consistent with the shape of the environment in **Fig. 11**.

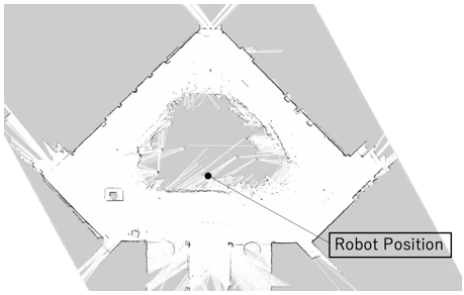


**Fig. 11. Courtyard map.**

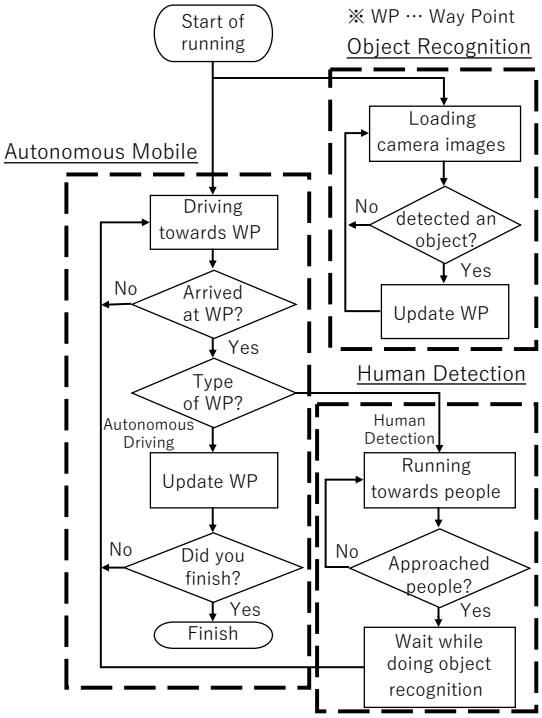


**Fig. 12. Flowchart of autonomous mobile.**

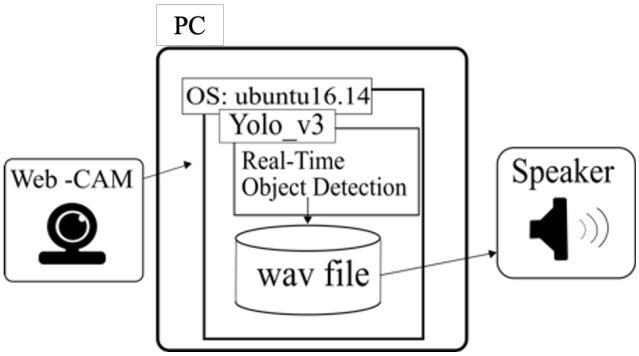


**Fig. 13. Overview of object recognition system.**

The follow-up performance of the uniaxial gimbal mechanism was also evaluated. First, the gimbal mechanism is tilted by sending a command value of 30 [deg] as the maximum angle that can be taken in the slope. Then, the command value of 0[deg] is input as the step input, and the gimbal's response time to reach the target is measured. This experiment was captured with a camera and the response time was calculated from the frame numbers. When the frame rate was 60 fps, the response time was 0.267 [s] as the system became static at 16 frames. The Navit(oo)n drives at 4 [km/h] of the maximum speed. We empirically evaluate the gimbal's performance of the self-localization, and verify this response time is sufficient by the following experiments.

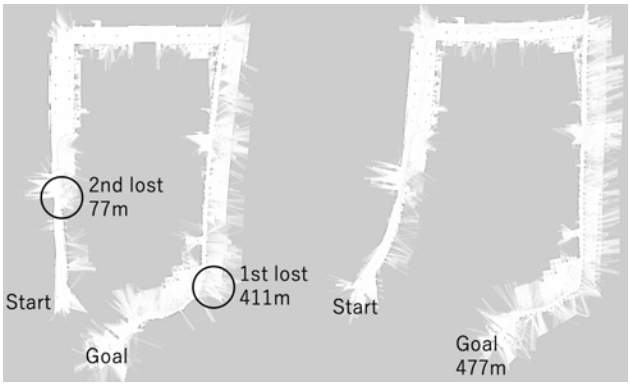


(a) 2019 (b) 2020

**Fig. 14. Generated map.**

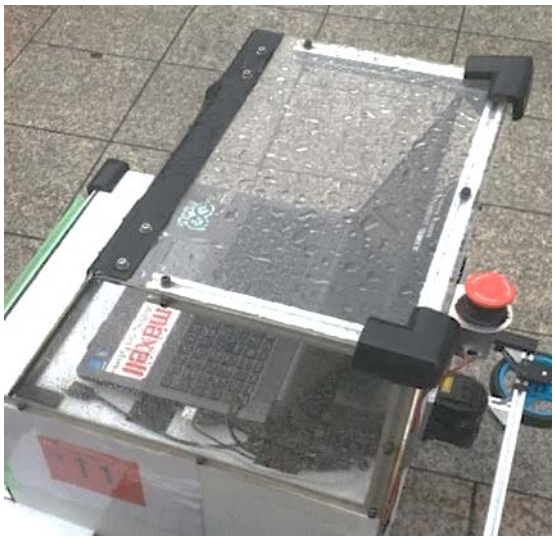

**Fig. 15. Photo of Navit(oo)n operating during rainfall.**

**Fig. 16. Ogimachi park hill.**

## 4. NAVIGATION SYSTEM

Navit(oo)n's ROS-based navigation system controls its displacement in the natural terrain. For the Nakanoshima Challenge, the system incorporated autonomous mobile, person detection, and object recognition. **Fig. 12** displays the relationships between these categories and the general flow process.

Note the flowchart is branch according to the waypoint at "Type of WP?" in **Fig. 12**, here, waypoint is an 2D coordinate point used in autonomous movement system. Basically, the flowchart is followed in autonomous mobile section in **Fig. 12**, but switches to the person detection section only when it approaches the waypoint of the person detection. The points for the detection are marked on the environment map in advance.

### 4.1. Autonomous driving

In this study, autonomous mobile involves the navigation stack in ROS, gmapping, move_base, and amcl packages[14, 15]. The flow comprises the following:

1) Creating an environment map, manually operating the robot once, running the entire route through a trial course, and saving the created map.

2) Designating the driving path, setting waypoints 1 m apart on the map by manually operating the robot again on the route. After completing placement of the waypoints, these are saved in CSV format.

3) Ensuring the autonomous mobile depends on the environmental map and the waypoints, so that the robot runs directly from one waypoint to the other until the goal is attained.

In the Nakanoshima Challenge, although we used move_base for route planning, the driving behavior faced difficulty stabilizing. Thus, in the Nakanoshima Extra Challenge, our route planning aimed to prolong the updating period and to maintain a stable tone. Moreover, as debugging heuristics, setting the running speed faster within a safe range was necessary.

### 4.2. Person Detection

To address the second problem stated in Section 2, LiDAR was used to measure the distances between the robot and the persons around it. For person detection, there are several methods proposed, such as using only cameras[16] and machine learning, or combining Lidar and cameras[17]. In the present study, the latter was adopted.

We extracted several nearest points from the robot's front and calculated the average distance. A color-recognition camera, Pixy, enabled detection of each person's direction. Since the target person for recognition wore a distinctive orange vest, we examined the center of the orange object occupying the largest camera image area. We then adjusted the robot's posture to the person until the image's center coincided with that of the camera.

### 4.3. Object Recognition

To address the third problem stated in Section 2, we introduced real-time object recognition using a web camera based on Yolo_v3 [18-20]. **Fig. 13** displays the structure of Navit(oo)n's object recognition system, an independent system from the control PC.

The objects for discrimination included PET bottles, cans, and lunch boxes. The Yolo_v3 detects objects in real time, with the system playing an audio file prepared in advance through a speaker to the surrounding. To achieve the recognition tasks, we used the learned network of the template set and rewriting of the answer list.

## 5. Experiment

### 5.1. Nakanoshima Challenge

The Nakanoshima Challenge occurred on September 23rd, 2019, with the uniaxial gimbal mechanism on Navit(oo)n still undeveloped. We examined the proposed system in two actual runs. For the 1st run in the course distance of 477 m, Navit(oo)n covered 411 m before losing its positioning on the slope as shown in **Fig. 14(a)**, while person detection and garbage recognition were successful. For the 2nd run, Navit(oo)n covered 77 m and lost again on the slope.

The losses of self-localization are both attributed to the slope. If the LiDAR detects the ground, the robot misrecognizes its position because the measurement data differs from that in the prepared environmental map. As such, the particle dispersion approach in the amcl becomes large, and if the acceptable recovery range is exceeded, the robot loses the self-positioning characteristic.

Another possible cause of positioning loss is wheel idling. Since self-localization depends on wheel odometry, a rotating wheel while idling is considered as displacement by the robot. Such a situation explains the difference between the expected and actual positions. We also realized that the auxiliary wheels were very stiff, causing significant vibration of the robot on the track. This vibration adversely affects the navigation and requires improvement in the future.

Navit(oo)n was equipped with the uniaxial gimbal mechanism and participated again in the Nakanoshima Challenge on September 20th, 2020. Navit(oo)n covered the whole 477 m in the two runs, demonstrating the effectiveness of the gimbal mechanism. **Fig. 14 (b)** shows the environmental mapping result of 2020. The map of 2019 is similar to the real course than that of 2020, because the proposed gimbal system are working at a deformed world. However, both the map generation and autonomous navigation were performed in that world, and the slope problem was solved by the gimbal, thus we concluded that the better autonomous movement was achieved than the past one.

We also evaluated the robot's resistance to heavy rain by leaving it in operation during a typhoon on the challenge day. **Fig. 15** shows the photograph of the robot operating under rainfall.

**Fig. 17. Roads within the Ogimachi park with the robot in action.**

### 5.2. Nakanoshima Extra Challenge

The Nakanoshima Extra Challenge took place at the Ogimachi Park in Osaka, Japan, on December 8th, 2019. The Park's 861-m-long track contains longer slopes and more natural terrain than the Nakanoshima's. The abundant plants and trees in parks involve shape variations that are more complex than human-made structures, making autonomous mobile difficult. The Nakanoshima Extra Challenge also necessitated ascending a hill. Capturing the features of the hill using the 2D LiDAR was complicated by the simple surrounding. **Fig. 16** shows a test run of Navit(oo)n for hill climbing. However, during the actual run, the hill was not attempted because of limited time for debugging.

We evaluated the uniaxial gimbal mechanism in the Nakanoshima Extra Challenge. Of the 861 m involved, the robot covered 575 m before losing its positioning. The garbage recognition and person detection characteristics were not tested because these were proven in the Nakanoshima Challenge.

At the Ogimachi Park, the uniaxial gimbal mechanism was demonstrated to effectively operate in the natural environment, despite the increased distance and terrain difficulty than in the Nakanoshima Challenge, because the uniaxial gimbal mechanism reduces the false detection of the ground and increases the amount of information, which is considered to be effective. The loss of self-localization may be explained by accumulated wheel odometry errors during the run. In fact, the uneven track surface at the Ogimachi Park favors such error accumulation. Navit(oo)n lost its position after emerging from a road with many plant types (**Fig. 17**). The accumulation errors on the narrow path likely caused the

environmental map and LiDAR measurement data to mismatch from where the shape suddenly changed. From this experience, the results show that the uniaxial gimbal mechanism adapts to slope, while, a terrain with many features and involving sudden feature changes is still problematic.

## 6. Conclusion

In this study, we designed and built a robot named Navit(oo)n and participated in Nakanoshima Challenges. In the first challenge on 2019, the robot was unable to reach the goal because of the slope covering only 411 of the 475 m. The uniaxial gimbal mechanism installed to cope with the slope was tested at Nakanoshima Challenge on 2020, the robot reached the goal twice, both times demonstrating the proposed gimbals usefulness. The robot was also tested in the Nakanoshima Extra Challenge, with the robot travelling 575 m of the 861 m. We verified the uniaxial gimbal mechanism is cope with the natural terrain, especially the slope problem of the 2D LiDAR.

As the future improvement, we plan to introduce a GPS for comprehensively estimating positioning and implementing a map switching technique. Our research on such robot's proceeds and participation in other challenges is envisioned.

## Acknowledgements

This development research was supported by members who participated in the Nakanoshima Challenge. We express gratitude to them for welcoming and sharing their experiences and development stories with newcomers.

## References:

[1] R. Sakai, S. Katsumata, T. Miki, T. Yano, W. Wei, Y. Okadome, N. Chihara, N. Kimura, Y. Nakai, I. Matsuo, and T. Shimizu. "A mobile dual-arm manipulation robot system for stocking and disposing of items in a convenience store by using universal vacuum grippers for grasping items," Advanced Robotics, Vol.34, pp. 219–234, 2020.

[2] I. Matsuo, T. Shimizu, Y. Nakai, M. Kakimoto, Y. Sawasaki, Y. Mori, T. Sugano, S. Ikemoto, and T. Miyamoto. "Q-bot: heavy object carriage robot for in-house logistics based on universal vacuum gripper," Advanced Robotics, Vol.34, pp. 173-188, 2020.

[3] J. Shintake, V. Cacucciolo, D. Floreano, and H. Shea, "Soft robotic grippers." Advanced Materials Vol.30, pp. 1707035, 2018.

[4] T. Watanabe, K. Yamazaki, and Y. Yokokohji. "Survey of robotic manipulation studies intending practical applications in real environments -object recognition, soft robot hand, and challenge program and benchmarking-," Advanced Robotics, Vol.31, pp. 1114-1132, 2017.

[5] E. Brown, N. Rodenberg, J. Amend, A. Mozeika, E. Steltz, M. R. Zakin, H. Lipson, and H. M. Jaeger, "Universal robotic gripper based on the jamming of granular material," Proceedings of the National Academy of Sciences, Vol.107, pp. 18809-18814, Nov 2010 .

[6] J. R. Amend, Jr, E. Brown, N. Rodenberg, H. M. Jaeger, and H. Lipson., "A Positive Pressure Universal Gripper Based on the Jamming of Granular Material," IEEE, Vol.28, pp. 341–350, April 2012.

[7] J. Amend, N. Chang, S. Fakhouri, and B. Culley, "Soft Robotics Commerciali-zation: Jamming Grippers from Research of Product," Soft Robotics, Vol.3, pp. 213-222, 2016.

[8] M. Fujita, K. Tadakuma, H. Komatsu, E. Takane, A. Nomura, T. Ichimura, M. Konyo, and S. Tadokoro. "Jamming layered membrane gripper mechanism for grasping differently shaped-objects without excessive pushing force for search and rescue missions," Advanced Robotics, Vol.32, pp. 590-604, 2018.

[9] M. Fujita, S. Ikeda, T. Fujimoto, T. Shimizu, S. Ikemoto, and T. Miyamoto, "Development of universal vacuum gripper for wall-climbing robot," Advanced Robotics, Vol.32(6), pp. 283-296, 2018.

[10] T. Tomokazu, S. Kikuchi, M. Suzuki, and S. Aoyagi, "Vacuum gripper imitated octopus sucker-effect of liquid membrane for absorption," 2015 IEEE/RSJ International Conference on Intelligent Robots and Systems (IROS), pp. 2929-2936, 2015.

[11] K. Inoue, S. A. Rahok, and K. Ozaki, "Proposal and consideration of design policy for autonomous mobile robots in real world robot challenge," Journal of the Robotics Society of Japan, Vol.30, pp. 234-244, 2018, (in Japanese).

[12] T. Yoshida, K. Irie, E. Koyanagi, and M. Tomono, "An Outdoor Navigation Platform with a 3D Scanner and Gyro-assisted Odometry," Transactions of the Society of Instrument and Control Engineers, Vol.47, pp. 493-500, 2011, (in Japanese).

[13] N. Kimura, and J. Ota, "Unknown object detection using floor height map for mobile robotson indoor floor with non-horizontal partial areas," Journal of the Robotics Society of Japan, Vol.34, pp. 699-710, 2011, (in Japanese).

[14] S. Thrun, "Probabilistic robotics," Communications of the ACM 45.3, pp. 52-57, 2002.

[15] G. Grisetti, C. Stachniss, and W. Burgard, "Improved techniques for grid mapping with rao-blackwellized particle filters," IEEE transactions on Robotics 23.1, pp. 34-46, 2007.

[16] S. Nakamura, T. Hasegawa, T. Hiraoka, and Y. Ochiai, "Person searching through an omnidirectional camera using CNN in the tsukuba challenge," Journal of Robotics and Mechatronics Vol.30 No.4, pp. 540-551, 2018.

[17] Y. Kanuki, and N. Ohta. "Development of Autonomous Robot with Simple Navigation System for Tsukuba Challenge 2015," Journal of Robotics and Mechatronics, Vol.28 No.4, pp.432-440, 2016.

[18] J. Redmon, and A. Angelova,. "Real-time grasp detection using convolutional neural networks," 2015 IEEE International Conference on Robotics and Automation (ICRA) IEEE, 2015.

[19] R. Joseph, S. Divvala, R. Girshick, and A. Farhadi, "You only look once: Unified, real-time object detection," Proceedings of the IEEE conference on computer vision and pattern recognition, pp. 779-788, 2016.

[20] J. Redmon, and A. Farhadi, "Yolov3: An incremental improvement," arXiv preprint arXiv:1804.02767, 2018.

## Supporting Online Materials:

[A] Tsukuba challenge, https://www.tsukubachallenge.jp/2019/
[B] Nakanoshima challenge,
http://www.proassist.co.jp/nknsmchallenge.html
[C] Nakanoshima extra challenge,
http://www.proassist.co.jp/nknsmchallenge/extrachallenge.html
[D] DARPA urban challenge,
https://archive.darpa.mil/grandchallenge/gallery.html